Volume 14, Issue 4, 142437 (1-12)

Iranian Journal of Catalysis (IJC)

https://doi.org/10.57647/j.ijc.2024.1404.37

An effective, novel, and recyclable γ-Fe_2O_3@MoS_2@Zn as magnetic nanocatalyst in the unprecedented synthesis of mono- and bis-triazoles

Ghafar Noohi[1], Manouchehr Mamaghani[2,*], Iman Rezaei[2], Rogheyeh Hossein Nia[2]

[1]*Department of Chemistry, University Campus 2, University of Guilan, Rasht, Iran.*
[2]*Department of Organic Chemistry, Faculty of Chemistry, University of Guilan, Rasht, Iran.*

[*]**Corresponding author:** m-chem41@guilan.ac.ir

Original Research

Received:
16 May 2024
Revised:
15 July 2024
Accepted:
8 September 2024
Published online:
8 October 2024

© The Author(s) 2024

Abstract:

Triazoles are an important group that have active biological properties, and their synthetic platform and reactions have been fully investigated by many synthetic and medicinal chemists during the recent years. Magnetic nanocatalysts have recently been used in the design of many reactions, so in this method, an efficient, novel, and recyclable magnetic nanocatalyst γ-Fe_2O_3@MoS_2@Zn was synthesized by the reaction of premade γ-Fe_2O_3@MoS_2 and $ZnCl_2$ to furnish the desired nanocatalyst which was characterized by using FT-IR, XRD, SEM, EDX, TEM, mapping and VSM techniques. The catalyst was used in the synthesis of mono- and bis-triazoles by the reaction of thiosemicarbazide or butane-1,4-diyl-bis(hydrazinecarbimidothioate) with various arylaldehydes at room temperature and in ethanol/water (50:50) as solvent. This novel protocol gave the desired products excellent yields ($92-96\%$) and lower reaction times ($15-20$ min). The synthesized magnetic nanoparticles were comfortability separated from the reaction mixture by means of an external magnet and employed in six consecutive runs without any significant changes in its catalytic activity. The advantages of this current method are short reaction time, excellent efficiency, use of green solvent, magnetic nanocatalyst, and cost-effectiveness.

Keywords: Bis-triazole; Nanoparticle; Triazole; γ-Fe_2O_3; MoS_2; Zinc

1. Introduction

Triazole is a class of heterocyclic compounds that have various applications in different fields, including pharmaceuticals, agriculture, and materials science [1–5]. The presence of triazole rings in organic compounds provides unique properties, making them valuable in drug discovery and synthetic organic chemistry. Many triazole derivatives have shown promising biological activities, such as antimicrobial, antifungal, antiviral, and anticancer properties (Fig. 1) [5–9]. These compounds can act as enzyme inhibitors or receptor agonists/antagonists, making them potential candidates for the treatment of various diseases. In the field of agriculture, triazoles are widely used as fungicides to protect crops from fungal infections [9–14]. They inhibit the growth of fungi by interfering with their sterol biosynthesis pathway. Triazole-based fungicides have proven to be effective against a wide range of plant diseases and have contributed significantly to improving crop yields [15, 16].

Triazoles also find applications in materials science due to their unique electronic and optical properties. They can act as ligands in coordination chemistry or be incorporated into polymers to enhance their thermal stability or electrical conductivity. Additionally, triazole-based compounds have been utilized in the synthesis of dyes, pigments, and fluorescent probes [17–20]. The synthesis of triazoles can be achieved through various methods, including click chemistry reactions such as the Huisgen 1,3-dipolar cycloaddition

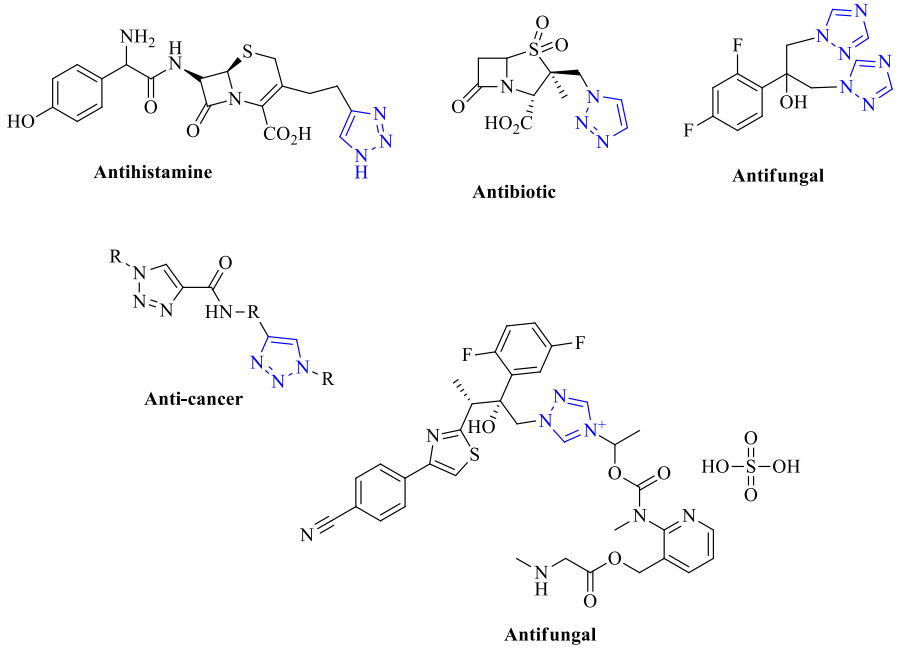

Figure 1. Some biologically active triazole derivatives.

reaction between an azide and an alkyne. This reaction has gained significant attention due to its efficiency and versatility in producing diverse triazole derivatives [21–23]. Various reaction conditions have been reported for the synthesis of triazoles such as using γ-Fe_2O_3@FAp@Cr [24] and Co [25] in ethanol, Fe_3O_4@SiO_2@Tannic acid [26] nanoparticles in $CHCl_3$, amino glucose-functionalized silica-coated $NiFe_2O_4$ MNPs in ethanol [27], [C_{16}MPy]$AlCl_3$Br in water [28], cobalt incorporated fluorapatite encapsulated iron oxide nanocatalyst in ethanol [29] and recently reported protocols on the synthesis and evaluation of functionalized triazoles [30–35]. Previously reported methods for the synthesis of triazole derivatives have some disadvantages, such as tough reaction conditions, intricate synthetic pathways as well as long reaction times with low yield. Thus, considering the importance of triazole derivatives, we decided to develop an effective and simple method for the preparation of mono- and bis-triazoles using a novel, green and recyclable nanocatalyst (γ-Fe_2O_3@MoS_2@Zn). Facile separation of the nanocatalyst from the reaction mixture, lower reaction time, excellent yields, and reusability of the catalyst are some prominent advantages of the present protocol.

2. Experimental

2.1 General

All chemicals were purchased from Merck and Fluka. Melting points were obtained on a Buchi B-545 apparatus in open capillary tubes. FT-IR spectra were recorded on a VERTEX 70 Brucker spectrometer using KBr pills. ^{1}H NMR spectra were run on a 300 MHz Bruker DRX-300 in DMSO-d_6 as solvent and TMS as internal standard. ^{13}C NMR spectra were done on a 75 MHz Bruker DRX-75 in DMSO-d_6 as solvent. The X-ray diffraction (XRD) pattern was carried out on a Philips X'Pert MPD diffractometer with a Co-Kα source (λ = 1.78897 $\AA$). Scanning Electron Microscope (SEM) was checked on a model VP 1450, company: LEO-Germany. Elemental analysis (EDX) was carried out on Oxford Instruments EDS Microanalysis X-MAX-80; model: TeScan-Mira III. TEM measurements were done on a Zeiss-EM10C-100 KV instrument, and the VSM spectrum was obtained on a BHV-55 vibrating sample magnetometer at room temperature. TLC was run in ethyl acetate: n-hexane (1:1) on Silica gel 60 F_{254} plates.

2.2 Synthesis of magnetic nanoparticles γ-Fe_2O_3@MoS_2@Zn

γ-Fe_2O_3@MoS_2 was synthesized according to the reported articles [31–33]. A mixture of γ-Fe_2O_3@MoS_2 (10 mg) in EtOH (10 mL) was irradiated by ultrasound (40 kHz) at 25 °C for 30 min, to give suspension I, then, 40 mmol $ZnCl_2$ was dissolved in 15 mL deionized water and then ammonia solution (4%) was added dropwise into the $ZnCl_2$ solution until the turbid solution was clear (solution II). Finally, solution II was mixed with suspension I, and the ultimate suspension was refluxed for 2 hours. The resulting product was removed using an external magnet 1.4 tesla, washed with hot water frequently, and dried at 100 °C for 6 hours in the oven to give γ-Fe_2O_3@MoS_2@Zn as a dark brown solid.

2.3 Typical procedure for the synthesis of mono- and bis-triazoles

Bis-triazole derivatives were synthesized according to the reported papers [24–29]. Briefly, a mixture of butane-1,4-diyl-bis(hydrazinecarbimidothioate) (1 mmol),

1-(4-nitrophenyl)-3-phenyl-1*H*-pyrazole-4-carbaldehyde (2 mmol) and γ-Fe_2O_3@MoS_2@Zn (7 mol%) were stirred in EtOH/ water (50:50) at room temperature and the progress of the reaction was monitored by TLC (ethyl acetate: n-hexane 1:1). After completion of the reaction, catalyst was removed by an external magnet, washed with ethanol and dried to be used in the next run. The solution was concentrated, and the obtained solid product was purified by recrystallization from ethanol to produce the desired product 3a with a 96% yield. The melting points of all known products were verified by comparing their melting temperature with the reported values [36, 37] (Table 4). The structure of new products (**3b**, **3c**, **5a**, **5b**, Tables 4&5) was established by FT-IR, ^{1}H NMR and ^{13}C NMR.

2.4 Physical and spectroscopic data of the novel compounds

2.4.1 2,2′-((butane-1,4-diylbis(sulfanediyl))bis(1h-1,2,4-triazole-5,3-diyl))bis(4-((e)-(3-nitrophenyl)diazenyl)phenol) (3b)

Yield 95%, Yellow solid; M. p. > 300 °C. FT-IR (KBr), ν, cm^{-1}: 3417 (OH), 3244, 3149 (NH), 2984 (C-H), 1588 (C=C and C=N), 1536, 1364 (NO_2), 1288 (C-S-C), 1218 (C-O). ^{1}H NMR (300 MHz, DMSO-d_6), δ, ppm: 1.80 (br. s, 2H), 3.10 (br. s, 2H), 7.07 (d, J = 9.0 Hz, 1H), 7.50-7.62 (m, 2H), 7.79-7.88 (m, 3H), 8.13 (s, 1H), 8.21 (s, 1H), 8.48 (s, 1H). ^{13}C NMR (75 MHz, DMSO-d_6), δ, ppm: 159.9, 152.5, 145.9, 139.0, 135.1, 131.2, 129.8, 124.6, 123.5, 122.7, 121.6, 117.3, 28.6, 26.2.

2.4.2 2,2′-((butane-1,4-diylbis(sulfanediyl))bis(1h-1,2,4-triazole-5,3-diyl))bis(4-((e)-(4-bromophenyl)diazenyl)phenol) (3c)

Yield 94%, Cream solid; M. p. > 300 °C. FT-IR (KBr), ν, cm^{-1}: 3445 (OH), 3313 (NH), 3151 (OH), 2931 (C-H), 1645, 1602, 1512 (C=C and C=N), 1263 (C-S-C), 1201 (C-O), 1059 (C-Br). ^{1}:H NMR (300 MHz, DMSO-d_6), δ, ppm: 1.71 (br. s, 2H), 3.01 (br. s, 2H), 6.99 (d, J = 9.0 Hz, 1H), 7.57 (d, J = 9.0 Hz, 2H), 7.72 (dd, J = 3.0, 9.0 Hz, 1H), 7.79 (d, J = 9.0 Hz, 2H), 8.04 (s, 1H), 8.12 (s, 1H), 8.38 (s, 1H). ^{13}C NMR (75 MHz, DMSO-d_6), δ, ppm: 160.1, 151.1, 145.8, 138.8, 135.6, 130.0, 129.7, 124.7, 124.3, 123.7, 121.7, 117.4, 29.9, 28.2.

2.4.3 5-(4-Chlorophenyl)-3-(cyclopentylthio)-1h-1,2,4-triazole (5a)

Yield 95%, Cream solid; M. p. 276-279 °C. FT-IR (KBr), ν, cm^{-1}: 3426, 3240 (N-H), 1601, 1511 (C=C and C=N), 1269, 1054 (C-O-C). ^{1}H NMR (300 MHz, DMSO-d_6), δ, ppm: 1.65-1.69 (m, 4H), 2.98 (t, J = 6.0 Hz, 4H), 3.2 (m, 1H), 7.39 (d, J = 8.5 Hz, 2H), 7.77 (d, J = 8.5 Hz, 2H), 11.41, (s, 1H, NH). ^{13}C NMR (75 MHz, DMSO-d_6), δ, ppm: 153.1, 135.9, 131.1, 129.5, 129.3, 128.6, 43.9, 35.4, 29.0.

2.4.4 3-(Cyclopentylthio)-5-(4-nitrophenyl)-1h-1,2,4-triazole (5b)

Yield 95%, Yellow solid; M. p. 291-294 °C. FT-IR (KBr), ν, cm^{-1}: 3372 (N-H), 1599, 1539 (C=C and C=N), 1507, 1338 (NO_2), 1225, 1059 (C-S-C). ^{1}H NMR (300 MHz, DMSO-d_6), δ, ppm: 2.43 (br. s, 4H), 3.2 (m, C-H), 3.83 (br. s, 4H), 7.60 (d, J = 8.4 Hz, 2H), 7.97 (d, J = 8.4 Hz, 2H), 8.86, (s, 1H, NH). ^{13}C NMR (75 MHz, DMSO-d_6), δ, ppm: 157.0, 135.2, 134.2, 131.1, 129.6, 129.1, 42.8, 24.9, 22.3.

3. Results and discussion

3.1 Preparation and characterization of the catalyst

γ-Fe_2O_3@MoS_2 was synthesized according to the recent reports [36–39]. Then, γ-Fe_2O_3@MoS_2 was suspended in EtOH (suspension I) and reacted with zinc chloride in NH_3 (4%) solution (suspension II) at 80 °C for 2 hours. The resulted γ-Fe_2O_3@MoS_2@Zn nanoparticles was purified by washing several times with deionized water (Scheme 1). The structure of the γ-Fe_2O_3@MoS_2@Zn was confirmed by FT-IR, XRD, EDX, Mapping analysis, SEM, TEM, and VSM techniques.

3.2 Characterization of γ-Fe_2O_3@MoS_2@Zn

3.2.1 Xrd

The XRD analysis of γ-Fe_2O_3@MoS_2@Zn magnetic nanoparticle is shown in Fig. 2. The XRD analysis shows diffraction peaks at around 2θ = 15.4°, 33.5°, 37.3° and 60.1°, which are related to the MoS_2 (JCPDS card No. 37-1492). Diffraction peaks at around 2θ = 31.8°, 34.9°, 39.6°, and 50.7° are also related to the γ-Fe_2O_3 (JCPDS File No. 79-0007). The average size of the nanomagnetic catalyst was calculated to be about 70 nm via the Scherrer equation.

Scheme 1.

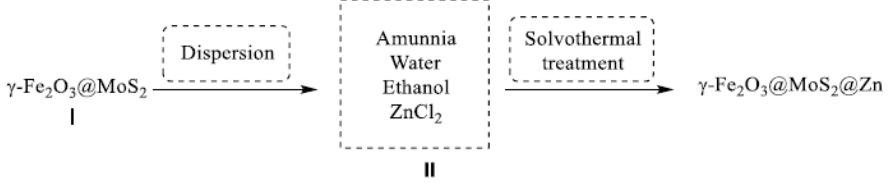

Scheme 1. A two-step solvothermal process for the preparation of the Fe_2O_3@MoS_2@Zn MNPs.

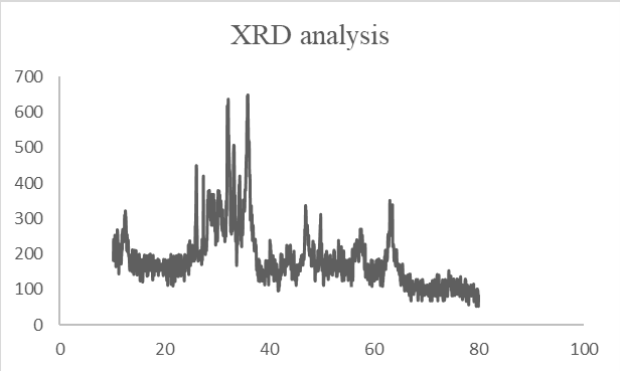

Figure 2. The XRD image of γ-Fe_2O_3@MoS_2@Zn.

3.2.2 SEM

The SEM image of the γ-Fe_2O_3@MoS_2@Zn MNPs were investigated and demonstrated via Scanning Electron Microscope technique (Fig. 3). According to the Scanning Electron Microscope images of synthesized magnetic nanocatalysts, the spherical morphology is confirmed for the nanocatalyst particles. The average size of γ-Fe_2O_3@MoS_2@Zn MNPs is about 75 nm.

3.2.3 EDX

The EDX (Fig. 4a) and mapping analyses (Figure. 4 b-g) for γ-Fe_2O_3@MoS_2@Zn nanocatalyst obviously confirmed the existence of Fe, O, Mo, S and Zn elements in the nanoparticles structure.

3.2.4 VSM

The morphology and size of the γ-Fe_2O_3@MoS_2 magnetic nanoparticles were obtained via the TEM analysis

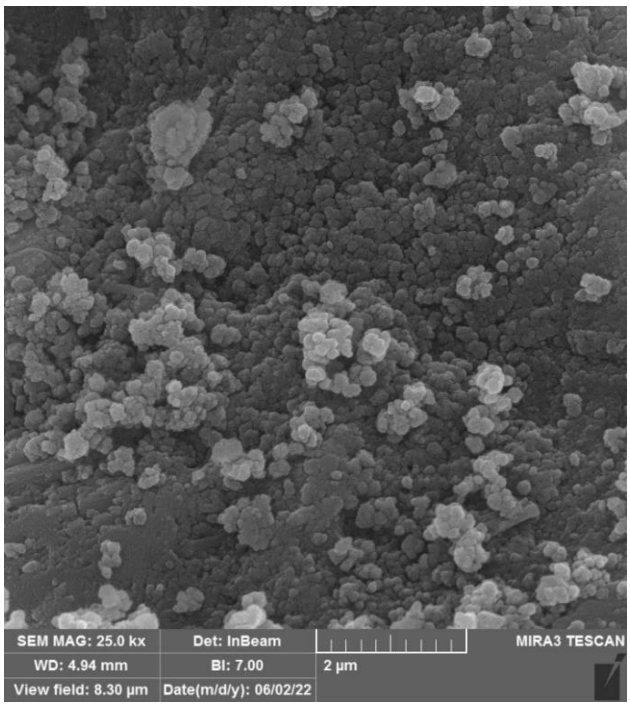

Figure 3. The SEM micrograph of the γ-Fe_2O_3@MoS_2@Zn magnetic nanoparticles.

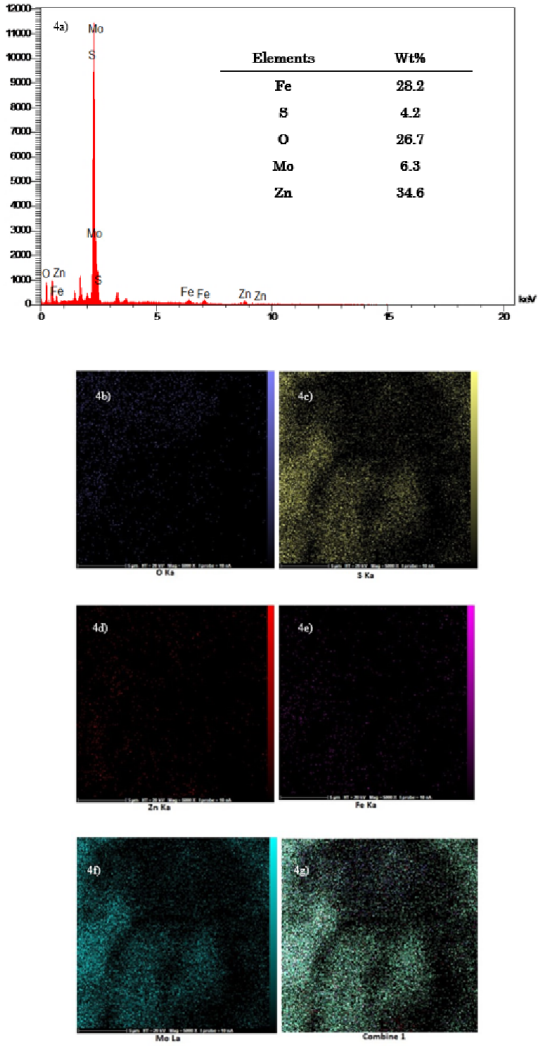

Figure 4. The EDX image (a) and mapping analysis (b) of γ-Fe_2O_3@MoS_2@Zn.

(Fig. 5). According to the TEM analysis, the size of the γ-Fe_2O_3@MoS_2@Zn nanoparticles was estimated at about $60-70$ nm.

3.2.5 FT-IR

The FT-IR spectrum of γ-Fe_2O_3@MoS_2@Zn nanocatalyst is shown in Fig. 6. The band at 576 cm^{-1} belongs to the stretching vibration of Fe-O, and the stretching vibration of Mo-O appears at 1021 cm^{-1}. The broad band at 3288 cm^{-1} is related to the stretching vibrations of the hydroxide groups and adsorbed water [36–38].

3.2.6 VSM

Fig. 7 clearly shows the magnetic properties of γ-Fe_2O_3@MoS_2@Zn. The VSM curve of γ-Fe_2O_3@MoS_2@Zn MNPs was obtained using a vibrating sample magnetometer at 25 °C. The results confirmed that γ-Fe_2O_3@ MoS_2@Zn nanoparticles have superparamagnetic behavior at room temperature. The magnetic properties of γ-Fe_2O_3@MoS_2@Zn led to easy separation of the catalyst using an external magnet.

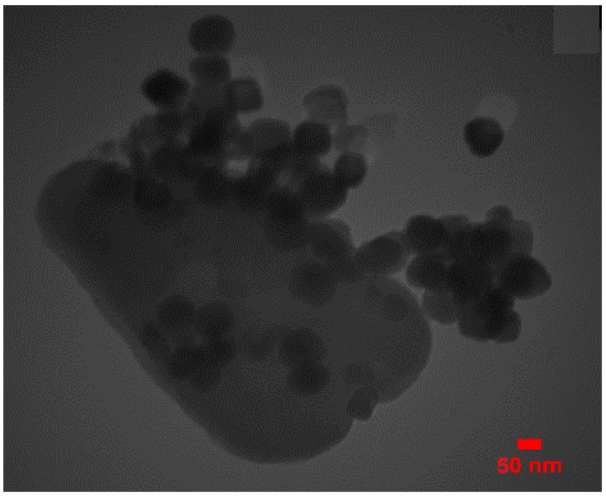

Figure 5. TEM spectra of γ-Fe_2O_3@MoS_2@Zn.

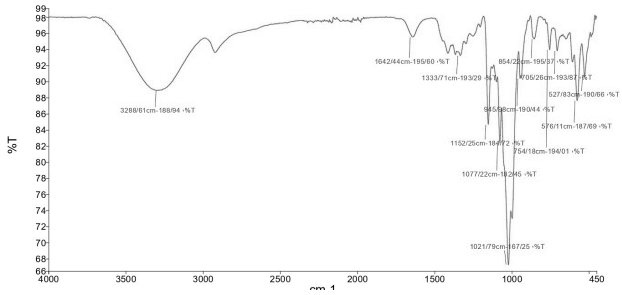

Figure 6. FT-IR spectra of γ-Fe_2O_3@MoS_2@Zn.

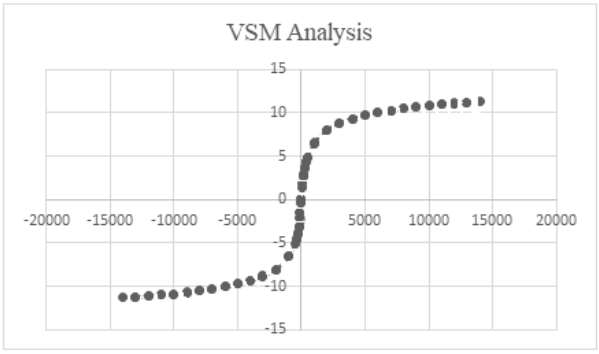

Figure 7. VSM analysis of γ-Fe_2O_3@MoS_2@Zn.

After preparation and characterization of the γ-Fe_2O_3@MoS_2@Zn MNPs via spectroscopic and microscopic techniques, its catalytic activity was examined by the synthesis of a series of mono- and bis-triazoles (Scheme 2). To optimize the reaction conditions, butane-1,4-diyl-bis(hydrazinecarbimidothioate) **(1)** and 1-(4-nitrophenyl)-3-phenyl-1*H*-pyrazole-4-carbaldehyde **(2a)** were reacted in the presence of γ-Fe_2O_3@MoS_2@Zn MNPs as a model reaction in diverse conditions by using different solvents and temperatures (Table 1).

The effect of various catalysts and solvents on the reaction time and yield was checked. The results showed that the reaction in EtOH/water (50:50) at room temperature in the presence of γ-Fe_2O_3@MoS_2@Zn nanocatalyst leads to product **3a** in 15 min and 96% yield (Table 1, Entry 8). The current method demonstrated that the reaction in the presence of γ-Fe_2O_3@MoS_2@Zn MNPs produces admissible results.

This method was compared with reported methods and

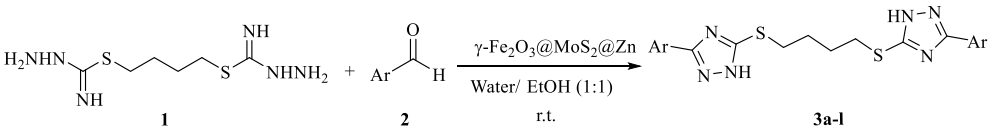

Scheme 2. Synthesis of the bis-triazole hybrids using γ-Fe_2O_3@MoS_2@Zn MNPs.

Table 1. Synthesis of **3a** by of γ-Fe_2O_3@MoS_2@Zn nanocatalyst in various solvents and temperatures.

Entry	Solvent	Temperature (°C)	Time (min)	Yield (%)[a,b]
1	EtOH	25	16	94
2	MeOH	25	17	91
3	Iso-propyl alcohol	25	19	86
4	t-BuOH	25	18	89
5	THF	25	25	67
6	Toluene	25	30	71
7	H_2O	25	18	93
8	H_2O/EtOH	25	15	96
9	H_2O/EtOH	50	15	96
10	H_2O/EtOH	80	15	96

[a]isolated yield. [b]Reaction conditions: butane-1,4-diyl-bis(hydrazinecarbimidothioate) 1 (1 mmol), 1-(4-nitrophenyl)-3-phenyl-1*H*-pyrazole-4-carbaldehyde **2a** (2 mmol), solvent (5 mL), catalyst (7 mol%).

different catalysts which showed that the current protocol provides a better result (Table 2).

The effect of the amount of nanocatalyst was examined on the progress of the model reaction by using various amounts of the catalyst and the results are presented in Table 3 which confirms that the use of 7 mol% of the catalyst produces the product **3a** in lower reaction time and higher yield (Table 3, Entry 2).

This method was utilized in the synthesis of a series of bis-triazole derivatives under the optimized reaction conditions, and the results are shown in Table 4.

The scope of this protocol was further extended to the reaction of cyclopentyl hydrazinecarbimidothioate (**5**) and arylaldehydes in EtOH/water (50:50) in the presence of γ-Fe_2O_3@MoS_2@Zn nanocatalyst and at room temperature which led to products **5a** and **5b** (Scheme 3) in excellent yields (Table 5). Our investigations showed that the reaction with aryl aldehydes bearing electron-withdrawing or electron donating group proceeds almost with similar efficiency. The advantages of this current method are short reaction time, excellent efficiency, use of green solvent, easily separable nanocatalyst, and cost-effectiveness.

The proposed mechanism for the synthesis of mono- and bis-triazoles catalyzed by γ-Fe_2O_3@MoS_2@Zn is demonstrated in Scheme 4. Initially, carbonyl group of arylaldehyde is activated by γ-Fe_2O_3@MoS_2@Zn, then, butane-1,4-diyl-bis(hydrazinecarbimidothioate) or cyclopentyl hydrazinecarbimidothioate is added to the activated carbonyl group which leads to the intermediates (A) and (B). In continuation, the target products **3a-l, 5a**, and **5b** are formed by intramolecular cyclization.

Figure 8 shows the recyclability of γ-Fe_2O_3@MoS_2@Zn nanocatalyst in the synthesis of model compound **3a**. After

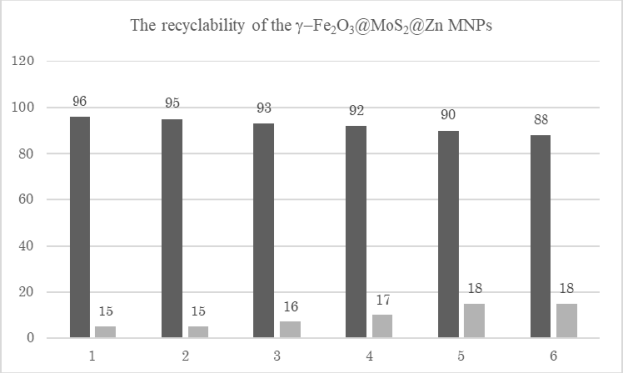

Figure 8. The recyclability of γ-Fe_2O_3@MoS_2@Zn for the preparation of target product **3a**.

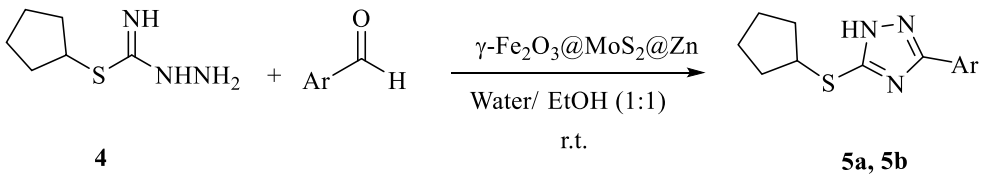

4 **5a, 5b**

Scheme 3. Synthesis of the mono-triazole derivatives by γ-Fe_2O_3@MoS_2@Zn MNPs.

Table 2. Synthesis of **3a** via reported methods and current method.

Entry	Solvent	Temperature (°C)	Time (min)	Yield (%)[a,b]	Reference	
1	γ-Fe_2O_3@FAp@Co	EtOH	r. t.	55	95	[29]
2	γ-Fe_2O_3@FAp@Cr	EtOH	r. t.	60	94	[24]
3	γ-Fe_2O_3@FAp	EtOH/water	r. t.	95	90	
4	$ZnCl_2$	EtOH/water	r. t.	180	82	
5	γ-Fe_2O_3@MoS_2@Zn	EtOH/water	r. t.	15	96	Current method

[a]Isolated yield. [b]Reaction conditions: butane-1,4-diyl-bis(hydrazinecarbimidothioate) **1** (1 mmol), 1-(4-nitrophenyl)-3-phenyl-1*H*-pyrazole-4-carbaldehyde **2a** (2 mmol), solvent (5 mL), room temperature.

Table 3. Considering the effect of the amount of catalyst on the effect and reaction time of product **3a** in EtOH/water (50:50) solvent and at room temperature.

Entry	amount of catalyst (mol%)	Time (min)	Yield (%)
1	5	20	92
2	7	15	96
3	10	15	96

[a]Isolated yield. [b]Reaction conditions: butane-1,4-diyl-bis(hydrazinecarbimidothioate) 1(1 mmol), 1-(4-nitrophenyl)-3-phenyl-1*H*-pyrazole-4-carbaldehyde **2a** (2 mmol), solvent (5 mL), room temperature, catalyst 7 mol%.

Table 4. Synthesis of Bis-triazole hybrids (**3a-l**) using γ-Fe_2O_3@MoS_2@Zn magnetic nanoparticles under optimized conditions.

Entry	product	structure	Time (min)	M.P (Observed)	M.P (reported)	Yield[a] (%)
1	**3a**	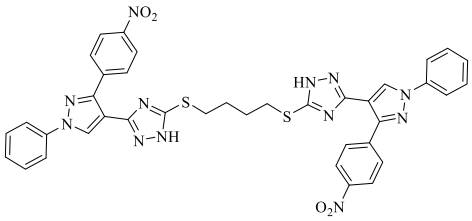	15	257-260	260-262[29]	96
2	**3b**	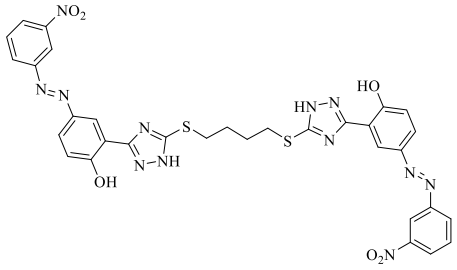	15	> 300	new	95
3	**3c**	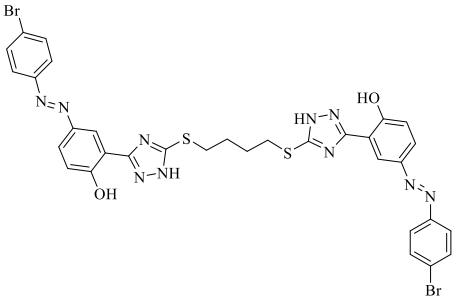	15	> 300	new	94
4	**3d**	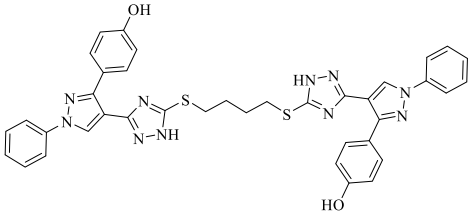	10	231-232	228-230[29]	93
5	**3e**	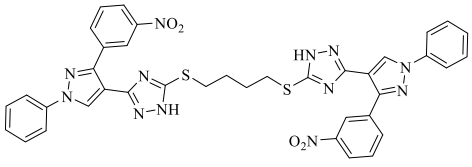	12	245-247	248-250[29]	92
6	**3f**	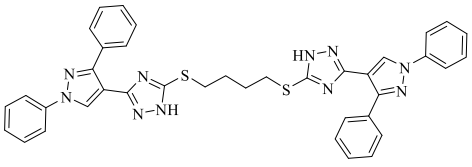	15	248-251	246-248[29]	95

[a]Isolated

Continue of Table 4.

Entry	product	structure	Time (min)	M.P (Observed)	M.P (reported)	Yield[a] (%)
7	**3g**	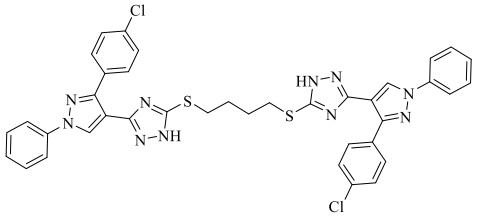	12	233-235	234-236[29]	95
8	**3h**	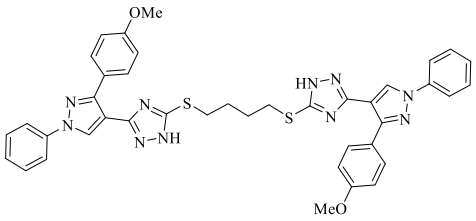	15	214-216	216-218[29]	94
9	**3i**	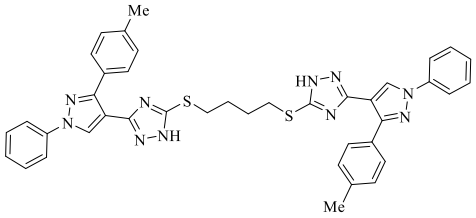	12	211-213	208-210[29]	92
10	**3j**	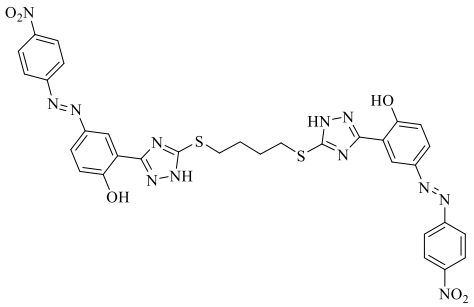	15	245-248	244-246[29]	96
11	**3k**	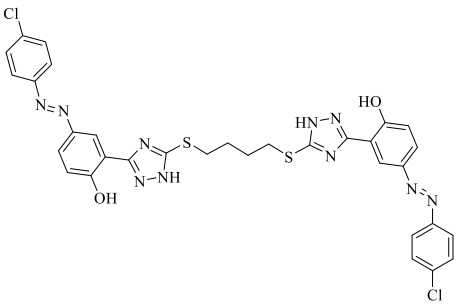	15	282-285	281-283[29]	95
12	**3l**	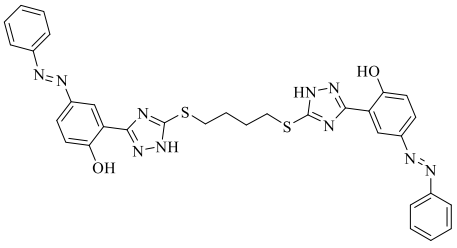	15	275-277	278-280[29]	95

[a]Isolated

Table 5. Synthesis of mono-triazole derivatives (**5a, 5b**) by γ-Fe_2O_3@MoS_2@Zn nanocatalyst.

Entry	product	structure	Time (min)	M.P (Observed)	M.P (reported)	Yield[a] (%)
1	**5a**	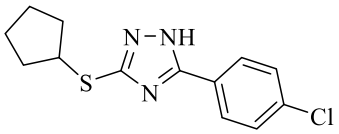	18	276-279	new	95
3	**5b**	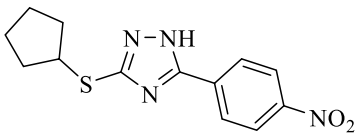	15	291-294	new	95

[a]Isolated yield

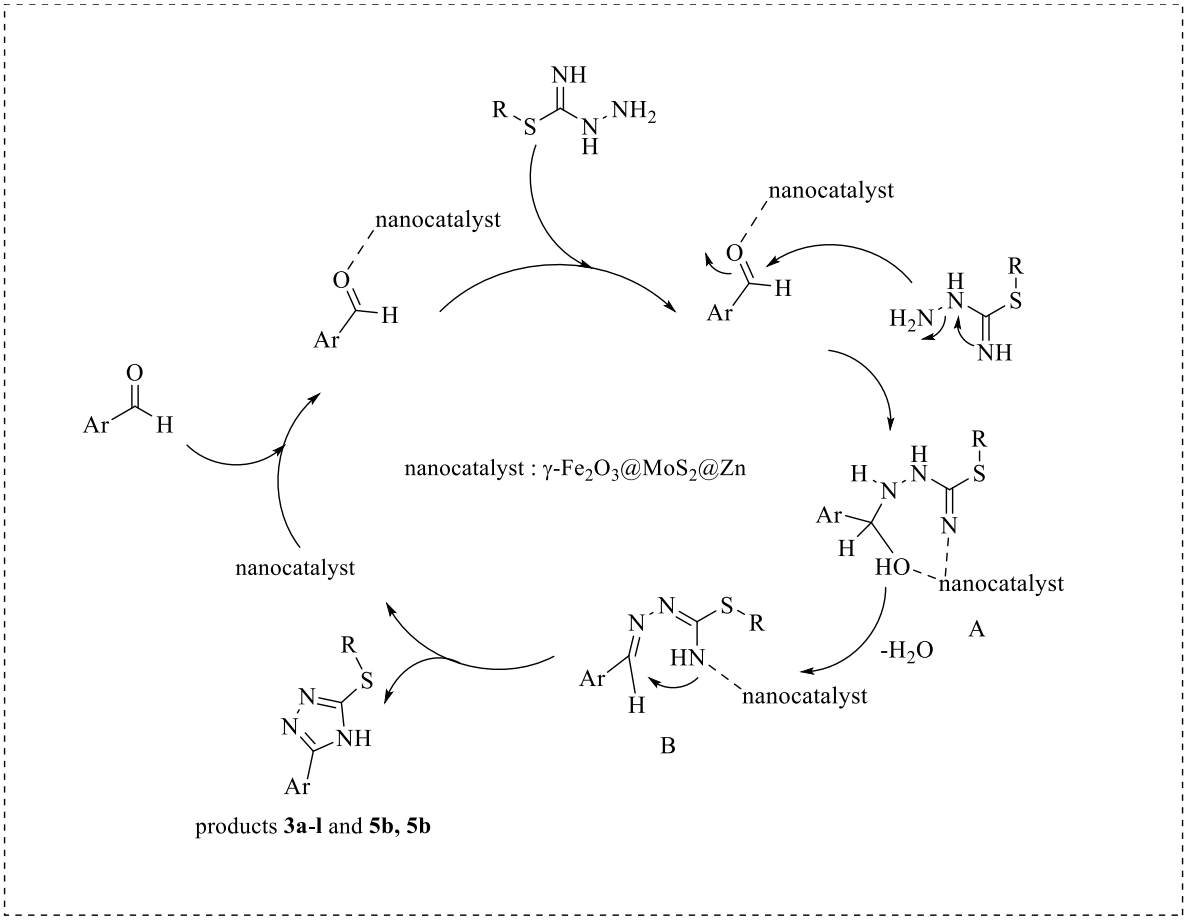

Scheme 4. The probable mechanism for the synthesis of mono- and bis-triazole hybrids catalyzed by γ-Fe_2O_3@MoS_2@Zn.

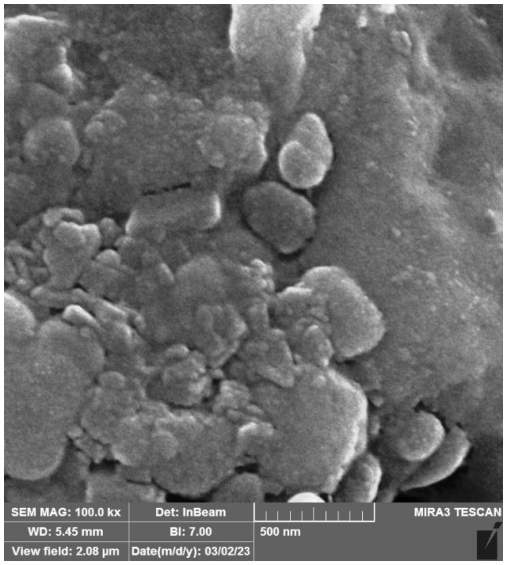

Figure 9. TEM image of γ-Fe_2O_3@MoS_2@Zn after six runs.

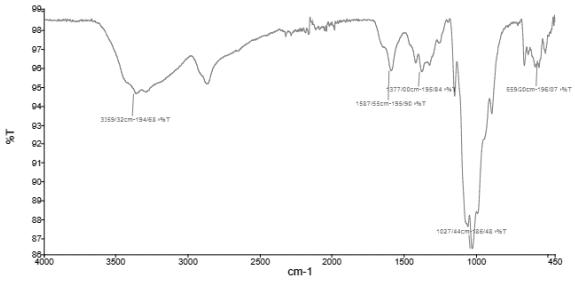

Figure 10. FT-IR image of γ-Fe_2O_3@MoS_2@Zn after six runs.

the end of each reaction, the nanocatalyst was separated from the reaction mixture using an external magnet, then washed with hot water, dried at 100 °C and reused in the subsequent run. This study showed that the catalytic activity and morphology of γ-Fe_2O_3@MoS_2@Zn nanocatalyst was mainly preserved after six repeated runs which was confirmed by SEM and FT-IR spectra (Figure 9 and Figure 10).

4. Conclusion

In present report, we have provided γ-Fe_2O_3@MoS_2@Zn as an efficient, novel, eco-friendly, recyclable magnetic nanoparticle for the synthesis of a series of mono- and bis-triazole derivatives. Among the evident advantages of the current method are remarkable reaction yield, short reaction time, simple purification of all products without the need for chromatographic separation and easy recyclability of the catalyst.

Acknowledgment
The authors gratefully acknowledge partial financial support from the Research Council of the University of Guilan.

Authors Contributions
Authors were equally contributed in acquisition and analysing the data as well as preparing the paper.

Availability of Data and Materials
Data is available on request from the corresponding author, upon reasonable request.

Conflict of Interests
The authors declare that they have no known competing financial interests or personal relationships that could have appeared to influence the work reported in this paper.

Open Access
This article is licensed under a Creative Commons Attribution 4.0 International License, which permits use, sharing, adaptation, distribution and reproduction in any medium or format, as long as you give appropriate credit to the original author(s) and the source, provide a link to the Creative Commons license, and indicate if changes were made. The images or other third party material in this article are included in the article's Creative Commons license, unless indicated otherwise in a credit line to the material. If material is not included in the article's Creative Commons license and your intended use is not permitted by statutory regulation or exceeds the permitted use, you will need to obtain permission directly from the OICC Press publisher. To view a copy of this license, visit https://creativecommons.org/licenses/by/4.0.

References

[1] I. A. Al-Masoudi, Y. A. Al-Soud, N. J. Al-Salihi, and N. A. Al-Masoudi. *Chem. Heterocycl. Compd.*, **42**(2006):1377–1403. DOI: https://doi.org/10.1007/s10593-006-0255-3.

[2] M. M. Pearson, D. Rogers, J. D. Cleary, and S. W. Chapman. *Ann Pharmacother*, **37**(2003):420–432. DOI: https://doi.org/10.1345/aph.1C261.

[3] N. D. Greer. *Bayl. Uni. Med. Cent.*, **20**(2007):188–196. DOI: https://doi.org/10.1080/08998280.2007.11928283.

[4] I. A. Gural'skiy, V. A. Reshetnikov, I. V. Omelchenko, A. Szebesczyk, E. Gumienna-Konteckac, and I. O. Fritskya. *J. Mol. Struct.*, **1127**(2017):164–168. DOI: https://doi.org/10.1016/j.molstruc.2016.07.094.

[5] Y. L. Fan, X. Ke, and M. Liub. *J. Heterocycl. Chem.*, **55**(2018):791–802. DOI: https://doi.org/10.1002/jhet.3112.

[6] N. Süleymanoğlu, R. Ustabaş, S. Direkelc, Y. B. Alpasland, and Y. Ünvere. *J. Mol. Struct.*, **1150**(2017):82–87. DOI: https://doi.org/10.1016/j.molstruc.2017.08.075.

[7] R. Kharb, P. C. Sharma, and M. S. Yar. *J. Enzyme. Inhib. Med. Chem.*, **26**(2017):1–21. DOI: https://doi.org/10.3109/14756360903524304.

[8] Y. Q. Hu, S. Zhang, Z. Xu, Z. S. Lv, M. L. Liu, and L. S. Feng. *Eur. J. Med. Chem.*, **140**(2017):335–345, . DOI: https://doi.org/10.1016/j.ejmech.2017.09.050.

[9] B. M. Chougala, S. Samundeeswari, M. Holiyachi, L. A. Shastri, S. Dodamani, S. Jalalpure, S. R. Dixit, S. D. Joshi, and V. A. Sunagar. *Eur. J. Med. Chem.*, **125**(2017):101–116. DOI: https://doi.org/10.1016/j.ejmech.2016.09.021.

[10] N. Fu, S. Wang, Y. Zhang, C. Zhang, D. Yang, L. Weng, B. Zhao, and L. Wang. *Eur. J. Med. Chem.*, **136**(2017):596–602. DOI: https://doi.org/10.1016/j.ejmech.2017.05.001.

[11] K. M. Banu, A. Dinakar, and C. Anantha-narayanan. *Indian J. Pharm. Sci.*, **61**(1999): 202–205. URL https://www.ijpsonline.com/articles/synthesis-characterization-antimicrobial-studies-and\pharmacological-screening-of-some-substituted-\123triazoles.pdf.

[12] L. Z. Chen, W. W. Sun, L. Bo, J. Q. Wang, C. Xiu, W. J. Tang, J. B. Shi, H. P. Zhou, and X. H. Liu. *Eur. J. Med. Chem.*, **138**(2017):170–181. DOI: https://doi.org/10.1016/j.ejmech.2017.06.044.

[13] J. Akhtar, A. A. Khan, Z. Ali, R. Haider, and M. S. Yar. *Eur. J. Med. Chem.*, **125**(2017):143–189. DOI: https://doi.org/10.1016/j.ejmech.2016.09.023.

[14] R. Gujjar, A. Marwaha, J. White, L. White, S. Creason, D. M. Shackleford, J. Baldwin, W. N. Charman, S. Buckner, F. S. Charman, P. K. Rathod, and M. A. Phillips. *J. Med. Chem.*, **52**(2009):1864–1872. DOI: https://doi.org/10.1021/jm801343r.

[15] Y. Q. Hu, C. Gao, S. Zhang, L. Xu, Z. Xu, L. S. Feng, X. Wu, and F. Zhao. *Eur. J. Med. Chem.*, **139**(2017):22–47, . DOI: https://doi.org/10.1016/j.ejmech.2017.07.061.

[16] A. Duran, H. N. Dogan, and H. Rollas. *Farmaco*, **57**(2002):559–564. DOI: https://doi.org/10.1016/S0014-827X(02)01248-X.

[17] X. Wen, Y. Zhou, J. Zeng, and X. Liu. *Curr. Topics. Med. Chem.*, **20**(2020):1441–1460. DOI: https://doi.org/10.2174/1568026620666200128143230.

[18] H. Wamhoff. *Compr. Heterocycl. Chem.*, **5**(1984):669–732. DOI: https://doi.org/10.1016/B978-008096519-2.00079-5.

[19] Y. M. Wu, J. Deng, X. Fang, and Q. Y. Chen. *J. Fluorine Chem.*, **125**(2004):1415–1423. DOI: https://doi.org/10.1016/j.jfluchem.2004.02.016.

[20] M. Whiting, J. Muldoon, Y. C. Lin, S. M. Silverman, W. Lindstrom, A. J. Olson, H. C. Kolb, M. G. Finn, K. B. Sharpless, J. H. Elder, and V. V. Fokin. *Angew. Chem.*, **45**(2006):1435–1439. DOI: https://doi.org/10.1002/anie.200502161.

[21] H. U. Reissig and F. Yu. *Beilstein J. Org. Chem.*, **19**(2023):1399–140. DOI: https://doi.org/10.3762/bjoc.19.101.

[22] C. W. Tornøe, C. Christensen, and M. Meldal. *J. Org. Chem.*, **67**(2002):3057–3064. DOI: https://doi.org/10.1021/jo011148j.

[23] V. V. Rostovtsev, L. G. Green and. Fokin, and K. B. Sharpless. *Angew. Chem., Int. Ed.*, **41**(2002): 2596–2599. DOI: https://doi.org/10.1002/1521-3773(20020715)41.

[24] K. K. Gangu, S. Maddila, S. N. Maddila, and S. B. Jonnalagadda. *Molecules*, **21**(2016):1281. DOI: https://doi.org/10.3390/molecules21101281.

[25] I. Rezaei and M. Mamaghani. *React. Kinet. Mech. Catal.*, **134**(2021):385–400, . DOI: https://doi.org/10.1007/s11144-021-02076-8.

[26] Z. Pourkarim and M. Nikpassand. *J. Mol. Struct.*, **1217**(2020):128433. DOI: https://doi.org/10.1016/j.molstruc.2020.128433.

[27] M. Nikpassand and M. J. Farshami. *J. Clust. Sci.*, **32**(2020):975–982. DOI: https://doi.org/10.1007/s10876-020-01855-y.

[28] J. D. Patil and D. M. Pore. *RSC Adv.*, **4**(2014):14314–14319. DOI: https://doi.org/10.1039/C3RA46916F.

[29] I. Rezaei and M. Mamaghani. *Current. Chem. Lett.*, **10**(2021):2220–2522, . DOI: https://doi.org/10.5267/j.ccl.2021.4.006.

[30] A. Abbas and K. M. Dawood. *Adv Heterocycl.Chem.*, **141**(2023):209–273. DOI: https://doi.org/10.1016/bs.aihch.2023.04.002.

[31] N. Korol, O. M. Holovko-Kamoshenkova, M. Slivka, O. Pallah, M. Y. Onysko, A. Kryvovyaz, N. V. Boyko, O. V. Yaremko, and R. Mariychuk. *Adv. Appl. Bioinforma. Chem.*, **16**(2023):93–102. DOI: https://doi.org/10.2147/AABC.S415961.

[32] A. Alibi, N. Elleuch, M. B. Hassen, S. Shova, F. Chabchoub, and M. Boujelbene. *J. Mol. Struct.*, (2024):139034. DOI: https://doi.org/10.1016/j.molstruc.2024.139034.

[33] X. B. Yang, C. H. Jia, X. Y. Miao, Y. C. Li, and S. P. Pang. *RSC adv.*, **13**(2023):2600–2610, . DOI: https://doi.org/10.1039/D2RA06646G.

[34] M. Tapera, H. Kekeçmuhammed, C. U. Tunc, A. U. Kutlu, I. Çelik, Y. Zorlu, O. Aydin, and E. Sarıpınar. *New J. Chem.*, **24**(2023):11602–11614. DOI: https://doi.org/10.1039/D3NJ01320K.

[35] Y. Cao, H. Huang, L. Wang, X. Lin, and J. Yang. *J. Org. Chem.*, **7**(2023):4301–4308. DOI: https://doi.org/10.1021/acs.joc.2c02879.

[36] M. Yin, Y. Wang, L. Yu, H. Wang, Y. Zhu, and C. Li. *J. Alloys. Compd.*, **829**(2020):154471. DOI: https://doi.org/10.1016/j.jallcom.2020.154471.

[37] K. Uma, E. Muniranthinam, S. Chong, T. C. K. Yang, and J. H. Lin. *Crystals*, **10**(2020):356–367. DOI: https://doi.org/10.3390/cryst10050356.

[38] X. Yang, H. Sun, L. Zhang, L. Zhao, J. Lian, and Q. Jiang. *Sci. Rep.*, **6**(2016):31591, . DOI: https://doi.org/10.1038/srep31591.

[39] F. Alavi, M. Mamaghani, and M. Sheykhan. *Polycycl. Aromat. Comp.*, (2023). DOI: https://doi.org/10.1080/10406638.2023.2254905.